Journal of Alloys and Compounds 952 (2023) 170018

Contents lists available at ScienceDirect

Journal of Alloys and Compounds

journal homepage: www.elsevier.com/locate/jalcom

Research article

Ti6Al4V coatings on titanium samples by sputtering techniques: Microstructural and mechanical characterization

Juan Carlos Sánchez-López [a,*], Marleny Rodríguez-Albelo [b], Miriam Sánchez-Pérez [a], Vanda Godinho [a,b], Carmen López-Santos [a,c], Yadir Torres [b]

[a] Instituto de Ciencia de Materiales de Sevilla (ICMS), CSIC-US, Avda. Américo Vespucio 49, E-41092 Sevilla, Spain
[b] Departamento de Ingeniería y Ciencia de los Materiales y del Transporte, Universidad de Sevilla, Escuela Politécnica Superior, Virgen de África 7, E-41011 Sevilla, Spain
[c] Departamento de Física Aplicada I, Escuela Politécnica Superior, Universidad de Sevilla, Virgen de África 7, E-41011 Sevilla, Spain

ARTICLE INFO

Article history:
Received 7 December 2022
Received in revised form 21 March 2023
Accepted 6 April 2023
Available online 7 April 2023

Keywords:
Magnetron sputtering
Titanium hard coatings
Hydrophobic behavior
Surface chemical functionalization
Wettability
Nanoroughness

ABSTRACT

Although titanium is widely used as biomaterial, the control of the interface properties between its surface and the surrounding physiological environment (like bone, other tissues or biofluids) results crucial to achieve a successful osseointegration and good biomechanical and functional performance. In this work, commercially pure titanium (Grade IV) discs obtained by conventional powder metallurgy were coated with 1–3 μm of Ti6Al4V (Grade V) alloy using DC-pulsed or high-power impulse magnetron sputtering (HiPIMS) technique with the aim of improving their biomedical performance. SEM, confocal microscopy, X-ray diffraction, nanoindentation and wetting measurements are used to evaluate the bio-interface role of the titanium-coated implants. Conformal Ti6Al4V coatings with controlled nano-roughness can be deposited with enhanced mechanical (H = 5–8 GPa; E = 140–160 GPa) and hydrophobic properties thanks to a dense columnar structure. The increased Ti-O bonding at the interface helps to prevent the corrosion due to the formation of a surface passivation layer. Particularly in the case of the HiPIMS process, the surface modification of titanium implants (chemistry, morphology and structure) appears as an effective strategy for satisfying the biomedical requirements and functionality, with enhanced mechanical properties and nanostructuration for prevention of bacteria colonization.

1. Introduction

Among the metallic biomaterials, titanium and its alloys have been preferentially applied for orthopedic and dental implants due to their excellent mechanical properties, high corrosion resistance and biocompatibility. Although low implant failure rates are reported, 5–10 % after up to 15 years, these numbers are considerable as in the last few decades the worldwide demand for long-lasting implants has strongly increased [1]. The success of most Ti-based implants, both dental and orthopedic, strongly depends on a proper osseointegration process. The osseointegration of an implant is a complex healing process ruled by a series of events, including the immune response of the patient, that starts as soon as the implant surface gets in contact with the patient body. One of the main reasons for the poor osseointegration of Ti and Ti based-alloys is their bio-inertness. Titanium surfaces form physical bonds with the bone tissue that are less stable than chemical osseous bonding, leading to an increased risk of implant loosening or failure in long-term [2]. Attention has been driven lately to surface modification strategies that could not only enhance or accelerate "bone-anchorage" by promoting a bio-interface between the implant and the bone tissue but also improve *in service* performance (mechanical properties and corrosion resistance). In this context, the strategies that are mostly used involve manipulation of roughness and texture of the implant surface, chemical and structural modification of the nature of the contact surface between the implant and the bone to promote a direct chemical bond [3], enhancing also physical factors such as bone anchoring, biomechanical stability and bone tissue guiding. In this sense several approaches have been used to locally manipulate the surface energy, biochemistry and topography of the implants [4–7] with the objective to facilitate the adhesion and differentiation of the bone-forming cells, which allows for the formation of a very convenient collagen matrix on the implant. At the same time, attention was paid to improve the mechanical properties of implants mainly focusing in increasing hardness and improving wear resistance of metallic implants [8]. The development of coatings,

* Corresponding author.
E-mail address: jcslopez@icmse.csic.es (J. C. Sánchez-López).

https://doi.org/10.1016/j.jallcom.2023.170018

conferring improved properties to the bulk implant, is an increasing research area with room for further developments of coating/substrate best candidate combinations leading to optimized properties for biomedical applications. In this optimization approach, magnetron sputtering is a very attractive plasma/vacuum-based deposition technique.

Plasma deposition techniques are characterized by a non-equilibrium physico-chemical environment that allows materials to be grown or modified at low temperature far from the thermodynamic limits. Magnetron sputtering is one of the most commonly employed plasma technologies in industry, for coating and surface modification, that allows for highly conformal coatings, well adherent to a broad variety of substrates. By controlling deposition parameters, surfaces of dense or porous coatings can be easily achieved, with control at the nano- and microscale of surface roughness, chemical composition and crystalline phases [9,10]. Moreover, plasma-based deposition methods result in highly reproducible coatings with sterile surfaces [11,12]. The described capabilities of the technique address some of the main challenges to be faced in the development of coating surfaces that will be in direct contact with the patient body. Primarily the coatings should present mechanical integrity and good adhesion to the substrate and be capable to withstand its insertion in the body and consequent mechanical loading. Within magnetron sputtering based techniques, HiPIMS is considered nowadays the preferred choice for improved mechanical, tribological and anticorrosive properties. It is reported that HiPIMS produces denser and smooth coatings with better uniformity in terms of film thicknesses on substrates with complex geometries when compared to direct current discharges (DC) [13,14]. This is surely an advantage in covering materials for implants with uniform dense structures and beneficial properties. The high pulse power densities achieved, in the order of 10^{18} e^-/m^3, at very small pulses (from microseconds to milliseconds) allow reaching very high degrees of ionization, 50–80 %, where more energetic atoms are deposited on the substrates when compared to the conventional DC discharges [15,16]. In DC sputtering the ionization degree is around 1–5 % and electronic densities of 10^{14} e-/m^3 are obtained that increase to 10^{16} e^-/m^3 when pulsed DC magnetron sputtering is employed [16–19]. The lower energy of the atoms arriving to the substrate gives origin to pronounced shadowing effects resulting in open intercolumnar porosity [16,20,21]. Nevertheless, only few recent works in literature are devoted to the preparation of coatings on implants [19,22–24] and, in particular, applied to powder metallurgy substrates.

Despite safety concerns [25,26], Ti6Al4V is still one of the most commonly employed titanium alloys in medical implants characterized by its good biocompatibility, mechanical and corrosion resistance properties. Over the last years, the manufacturing techniques for Ti6Al4V have been revised looking for procedures that could be easily improved in industry with shorter manufacturing times [27,28]. In this work we put together two well-known and well-established material preparation techniques in industry as powder metallurgy, to fabricate the implant substrate, and magnetron sputtering technique (specifically pulsed technologies), to modify the surface properties by coating deposition. This will enable the insertion of small implants to replace cortical bone tissues (e.g. after tumoral surgeries) with improved biofunctional and biomechanical surfaces. More specifically, the use of novel HiPIMS technique is explored for this purpose and compared with more conventional pulsed DC (DC-p) sputtering. The obtained results could open a new research niche with prospect to new coating possibilities and fast industrialization times.

2. Materials and methods

In this section, the fabrication and characterization of titanium substrates are firstly presented. The coatings deposition process is described below, as well as a detailed set of characterization techniques in order to evaluate the microstructure, thickness, homogeneity, wettability, and mechanical properties. This study will provide an insight of the behavior of the system (substrate plus coating) as a possible implant material.

2.1. Manufacturing and characterization of the commercially pure titanium (c.p.-Ti) substrates

Disk substrates (12 mm diameter and 4 mm height) of c.p.-Ti (grade IV) supplied by SEJOING Materials Co. Ltd. (Seoul, Korea), were manufactured by conventional powder metallurgy. The Ti powder was pressed at 1300 MPa using an Instron 5505 machine and sintered for densification in a molybdenum chamber furnace (Termolab, Agueda, Portugal) under high vacuum conditions ($\sim 10^{-5}$ mbar), at 1300 °C for 2 h. Before film deposition, the surface of the discs was carefully grounded and polished with a colloidal silica suspension.

2.2. Deposition of the Ti6Al4V coatings by magnetron sputtering

The coatings were deposited from Ti6Al4V targets (Grade V) from Photon Export of 2 in. of diameter and 3 mm of thickness. Silicon wafers (100) were also used for cross-section examination, determination of the coating thickness by scanning electron microscopy (SEM), phase composition by X-ray diffraction (XRD) and nanoindentation measurements. The base pressure of the vacuum chamber was $\approx 1 \times 10^{-4}$ Pa and the working pressure set at 0.75 Pa. A flux of 25 sccm of Ar was used for the sputtering process. DC-p and HiPIMS sources were employed to apply 250 W to the sputtering target during 150 min. The pulse conditions were 250 kHz and 89 % of duty cycle (DC-p) and 500 Hz and 2 % of duty cycle (HiPIMS). The substrate temperature was fixed at 250 °C. A working distance (distance substrate-target) of 10 cm was used for all coatings.

2.3. Phase composition, microstructural and mechanical characterization of coatings

The analysis of crystalline phase composition of the uncoated and coated specimens together with the target material used for deposition was carried out by XRD in an X′Pert Pro PANALYTICAL diffractometer in grazing incidence at 1°, using Cu Kα radiation.

The composition and chemical state of the coatings surface were determined by X-ray photoemission spectroscopy (XPS) in a PHOIBOS 100 spectrometer, working with pass energy of 15 eV and the Al Kα radiation as excitation source. Binding energy (BE) calibration of the spectra was performed assigning a BE of 284.5 eV to the C 1s peak due to adventitious carbon contamination.

To characterize the homogeneity, thickness, roughness and morphology of the coatings, images of the top-view and cross-section were acquired using SEM and confocal microscopy. A SEM-FEG Hitachi S4800 microscope operating at 5 kV was used for morphological and compositional analyses. The confocal microscopy images were taken at 50× magnification using a Sensofar S-Neox 090 microscope allowing the estimation of the surface roughness parameters in the uncoated and coated specimens. At least five different regions were analyzed for the estimation of the arithmetic surface roughness (S_a) in each sample.

The wettability was evaluated by the static contact angle (CA) measurements obtained with an OCA 20 Dataphysics instrument setup by depositing 2 µL microdroplets on the surface of the samples according to the Young's method. Measurements were done with water (pH 7) and bovine albumin serum (Sigma Aldrich), which form part and simulate the biological environment, respectively. The given CA value was obtained after averaging a minimum of 3 independent measurements per sample.

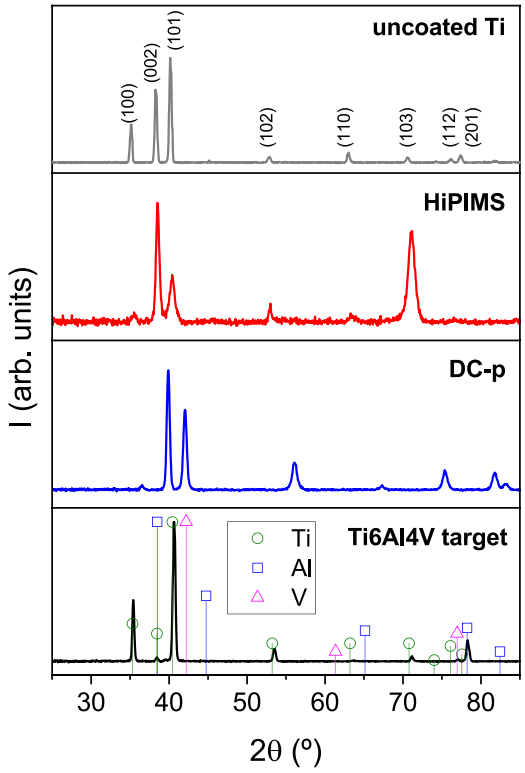

Fig. 1. XRD scans for the uncoated and coated titanium specimens. The diffractogram obtained for the target material is also included for comparison purposes. The positions of the crystalline phases of Ti (◯) (ICDD ♯1–1198); Al (□) (ICDD ♯4–0787) and V (△) (ICDD ♯1–1224) are marked in the target material and the crystallographic planes associated to the hexagonal hcp-Ti phase are noted on the uncoated specimen.

Nanoindentation experiments were performed with a KLA Nanoindenter G200X using the continuous stiffness measurement (CSM) technique with 50 mN of maximum load for the coatings and 500 mN for the c.p.-Ti substrate. All tests were carried out at room temperature with a diamond Berkovich (three-sided pyramid) indenter tip (< 20 nm). The load displacement data obtained were analyzed using the method of Oliver and Pharr [29] to determine the hardness and the elastic modulus as a function of the displacement of the indenter. The estimation of both properties was done in the region in which the indentation depth did not exceed 10–15 % of the coating thickness disregarding the initial points affected by tip defects and surface roughness. A 3 × 4 nanoindentation array was defined on the surface of each coating, with a 20 μm separation between consecutive indents to avoid effects from previous measurements. The CSM mode used and the number of indents in every sample allowed enough statistical data to obtain reliable and accurate results.

3. Results and discussion

The crystalline structure of the initial titanium substrates and coated specimens was examined by XRD in grazing incidence at 1°. Fig. 1 displays their corresponding diffractograms together with that of the Ti6Al4V target. The positions of the crystalline phases of Ti (ICDD #1–1198); Al (ICDD #4–0787) and V (ICDD #1–1224) are marked in the target material and the crystallographic planes associated to the hexagonal hcp-Ti phase are noted on the uncoated specimen. The positions of the peaks observed in both coatings are consistent with the hcp-Ti phase showing poorer crystallinity than the raw materials. The intensity ratios and the peak width vary depending on the type of sputtering deposition method used. Thus, the employ of HiPIMS conditions revealed to favor the growth of the (002) and (103) vs. (101) planes. The more energetic conditions of the HiPIMS plasmas lead to preferential orientation and lattice

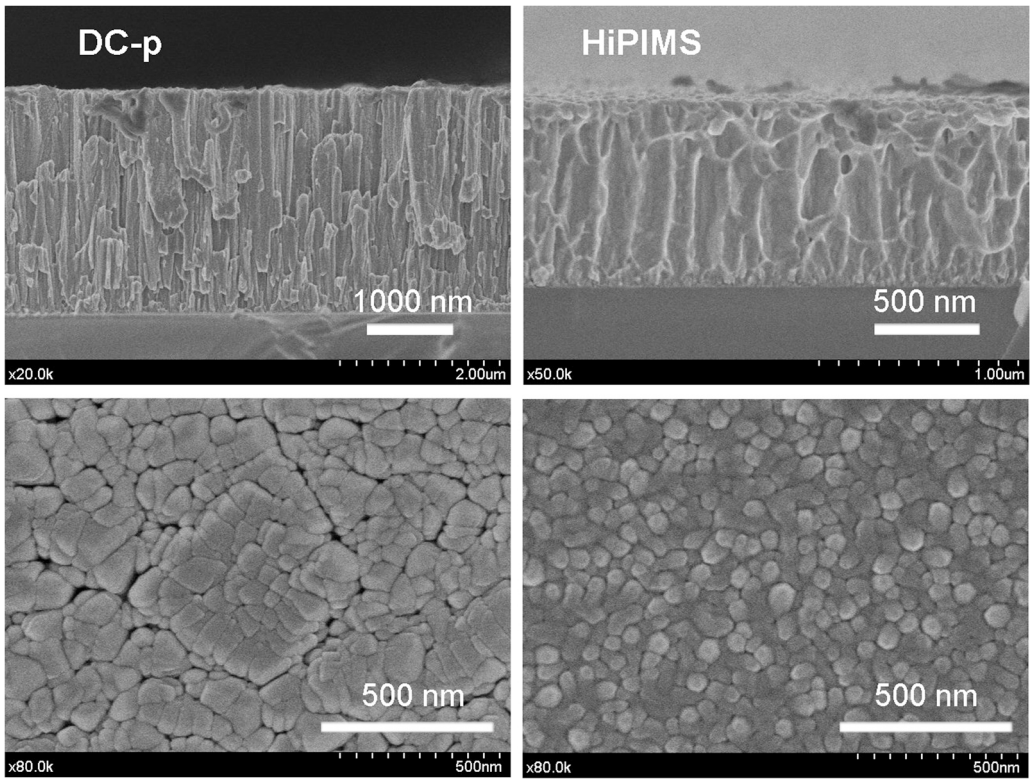

Fig. 2. SEM cross-section and planar view images of the DC-p and HiPIMS coatings. The percentage values (P_T %) represent the total porosity fraction estimated from the shown micrographs.

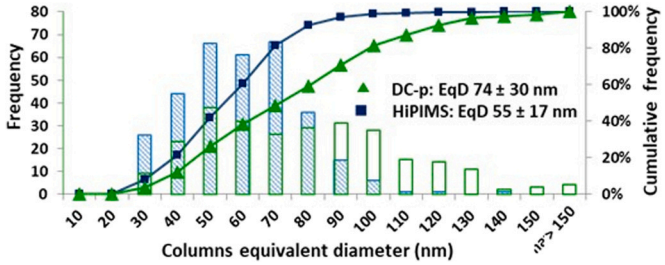

Fig. 3. Mean column size distribution for the DC-p and HiPIMS coatings.

distortion of crystalline planes induced by ion bombardment [30]. The observed peak broadening is indicative of a lower crystal size in agreement with the smaller columnar size evidenced by SEM (cf. Fig. 2).

Fig. 2 shows the SEM images (cross-section and top-view) of the coatings obtained by magnetron sputtering. These micrographs allow evaluating the thickness, morphology and compactness of the coatings obtained by DC-p and HiPIMS. The film are found to be conformal to the c.p.-Ti specimen with a homogeneous thickness on all substrate area of 2.70 ± 0.10 µm and 0.90 ± 0.05 µm for the DC-p and HiPIMS processes, respectively. The higher thickness obtained by the DC-p process is congruent with the lower deposition rates commonly obtained in HiPIMS processes [17]. This phenomenon is a consequence of the reduction of time when the pulse is on and the back-attraction of the higher fraction of positive target ions formed during the HiPIMS discharge [31]. The films grow developing a columnar morphology although they differ in the degree of compactness and intercolumnar porosity. The comparison of the planar and top view images denotes the differences in the column size and degree of packaging between DC-p and HiPIMS. The columns developed with the HiPIMS process are round and smaller leading to a higher density structure vs. more polygonal and heterogenous in the case of DC-p [15]. Fig. 3 displays the results obtained for a statistical analysis on these pictures confirming higher average mean column diameters and higher distribution in the DC-p sample. The equivalent mean diameter was found to be 55 ± 17 nm in HiPIMS vs. 74 ± 30 nm in DC-p. Considering a cumulative frequency of 80 %, the equivalent column diameters are lower than 70 nm in the HiPIMS while in the case of DC-p, the values extend towards 110 nm. Likewise, the porosity percentages (measured as the open intercolumn area in respect to the total surface) gave values of 0.9 % and 6.6 % for the HiPIMS and DC-p, respectively, indicative of a higher column compaction in the former case. This modification of the film microstructure is also consequence of the higher energetic conditions achieved in the HiPIMS discharge. The power delivered in the form of very short and intense pulses favors the increase of the ion flux and energies, which impinge the growing surface. In this context shadowing effects responsible by open intercolumnar porosity [13,15] are more important in the case of less energetic conditions of DC-p and a less compact columnar structure [20]. This is clearly illustrated in Fig. 2 (DC-p top view) where micropillars are formed by assembly of polygonal columns of different sizes, leaving open boundary regions.

Fig. 4 displays the optical micrographs and confocal images obtained for both type of coatings. The average arithmetic roughness (S_a) values of both coatings are compared with the initial values in a table include as inset. The average roughness values of both coatings obtained from confocal image analysis are rather low (below 50 nm in both cases) and similar to those measured for the initial substrates within the error deviations. This result denotes the high

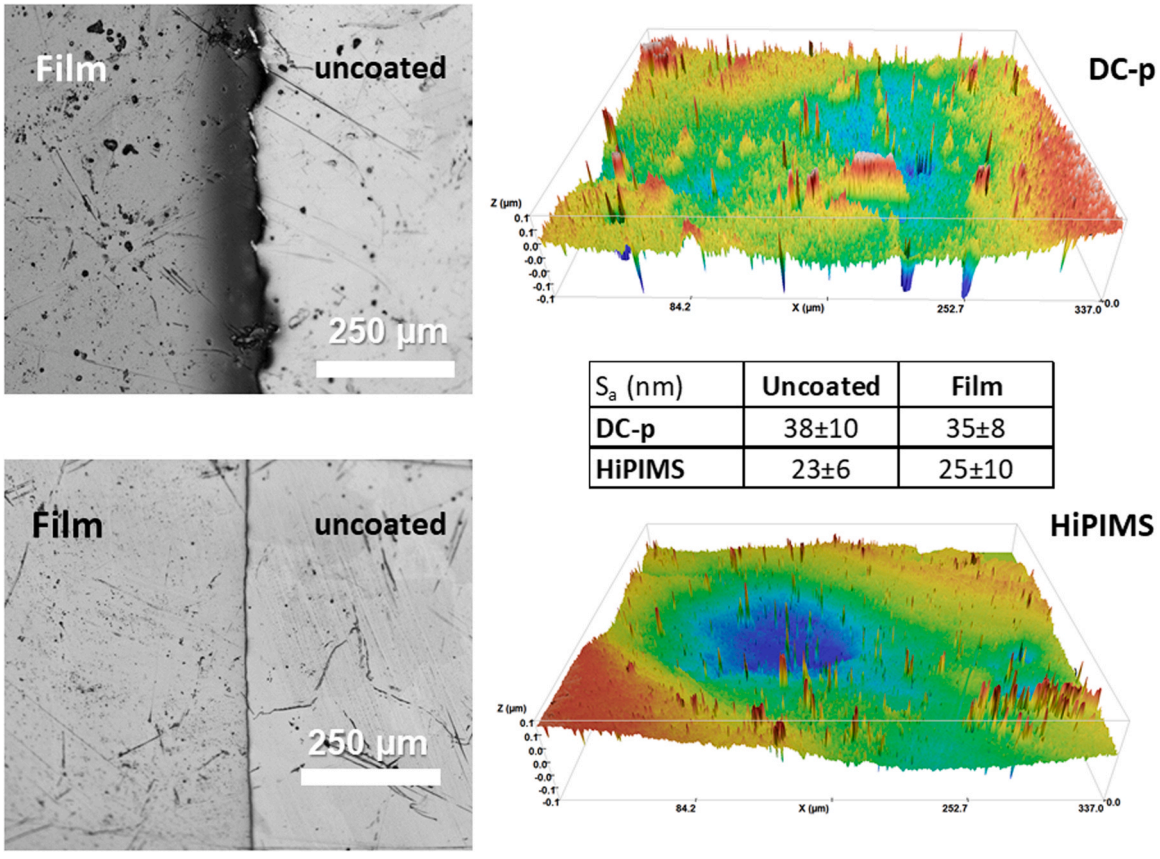

S_a (nm)	Uncoated	Film
DC-p	38±10	35±8
HiPIMS	23±6	25±10

Fig. 4. Optical pictures of the coating edge and confocal images obtained for the coated surfaces. The average roughness of the initial substrates and corresponding coatings are included as inset.

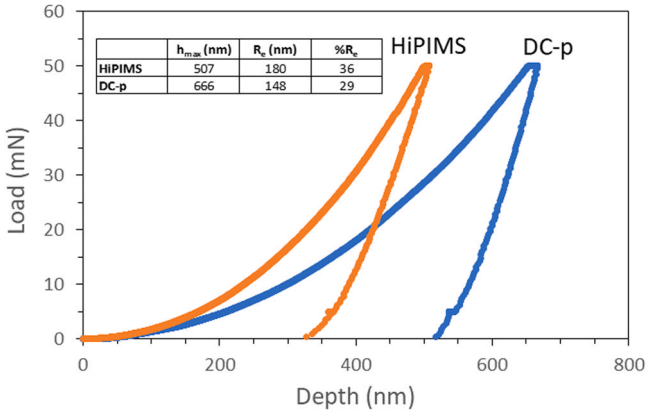

	h_{max} (nm)	R_e (nm)	%R_e
HiPIMS	507	180	36
DC-p	666	148	29

Fig. 5. Comparison between the load-displacement curves for the two types of TiAlV coatings: DC-p and HiPIMS.

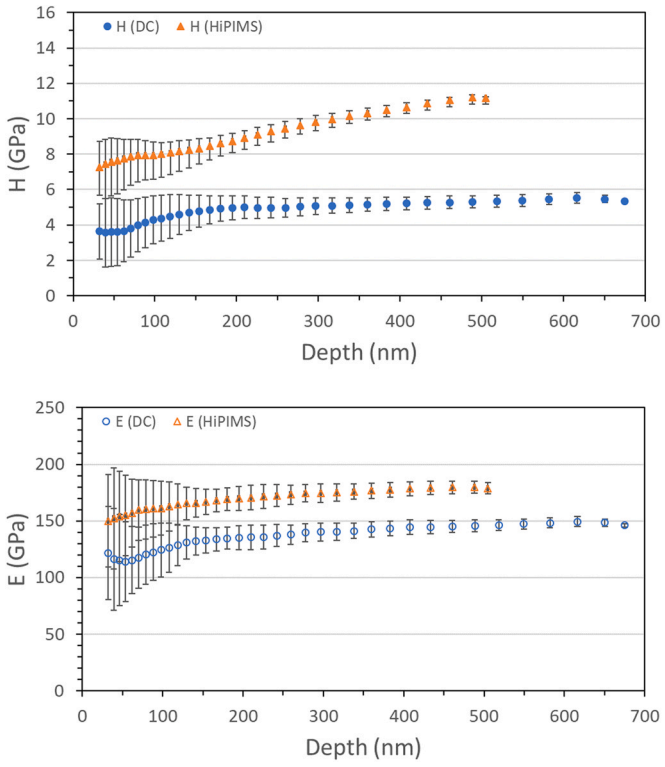

Fig. 6. Hardness and elastic modulus values for the DC-p and HiPIMS coatings.

conformability and film density achieved, characteristics of plasma assisted physical vapor deposition techniques [13,14].

The mechanical behavior of the coatings was studied using nanoindentation measurements at 50 mN of maximum load. Fig. 5 depicts the load-depth curves for HiPIMS and DC-p coatings and a summary of mechanical data obtained from them. Higher penetration depths are obtained with the DC-p sample indicating a lower nanohardness. A significant difference in elastic recovery is also noticed with 29 % and 36 % for the DC-p and HiPIMS (148 and 180 nm in absolute values), respectively. Another relevant feature is the pseudo-creep behavior during the holding time at maximum load for the DC-p film. This phenomenon has been already observed in thermal barrier layer coatings [32] and associated to potential slippage of the column boundaries. These differences in mechanical behavior are confirmed from the determination of the nanohardness and Young's modulus values (cf. Fig. 6 and Table 1), with

Table 1
Values corresponding to the Young's modulus, E, hardness, H, and the ratios H/E and H^3/E^2 measured by nanoindentation for the coated (DC-p, HiPIMS) considering the 1/10 rule and uncoated substrates (c.p.-Ti).

	E (GPa)	H (GPa)	H/E	H^3/E^2
DC-p	138 ± 9	5.0 ± 0.5	0.04	0.006
HiPIMS	161 ± 8	7.9 ± 0.7	0.05	0.019
c.p.-Ti*	176 ± 15	7.1 ± 1.2	0.04	0.011

*E and Vickers hardness (HV) values obtained by instrumented microindentation (P-h): E = 108 ± 5 GPa; HV0.10 = 441 ± 34 MPa

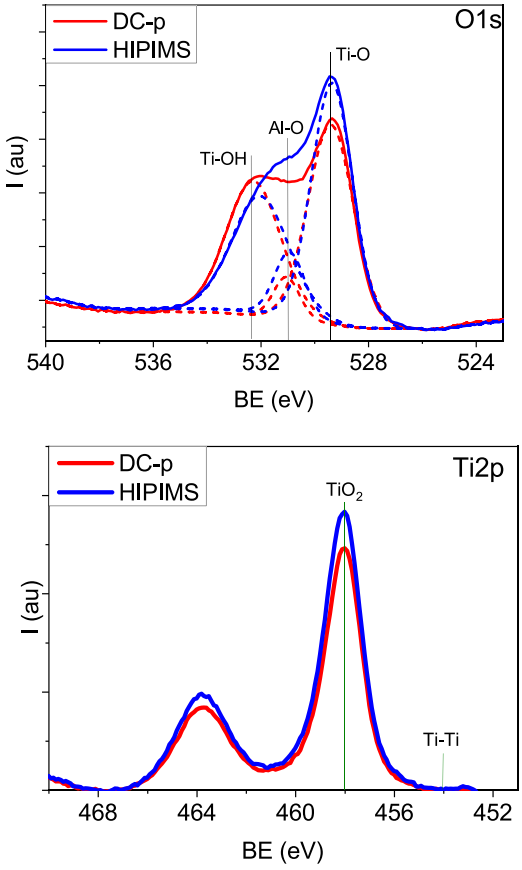

Fig. 7. - XPS O 1s deconvoluted photoelectron peaks and Ti 2p core level spectra for the DC-p and HiPIMS coatings. O 1s fitting is included as dot lines.

approximate values of 8 and 160 GPa (HiPIMS) and 5 and 140 GPa (DC-p), respectively. Table 1 resumes the mechanical properties in comparison with the uncoated c.p.-Ti specimen, including also the H/E ratio, which is related to the elastic strain to failure and wear resistance, and the H^3/E^2 ratio related to the resistance to plastic deformation [8,33]. The enhancement of the mechanical properties for the HiPIMS coating agrees with the changes observed previously in the film texture and morphology by XRD and SEM [34,35]. The higher intensity of the (103) peak in XRD was earlier observed for Ti alloys with improved hardness [34]. While the changes in film density rendered by the higher process energy were previously reported by Samuelsson et al. [35], estimating a density difference of ~15 % by RBS results. The H/E and H^3/E^2 values for the HiPIMS coating are similar to those reported in literature for laser treated Ti6Al4V alloy with improved anti-wear properties [36]. These results point out that coated surfaces by means of HiPIMS lead to improved mechanical and anti-wear properties compared to the native substrate, which play a significant role on the "in service" implant. The lower H and E values obtained for DC-p coating in respect to the bare substrate is associated to the heterogeneous microstructure formed

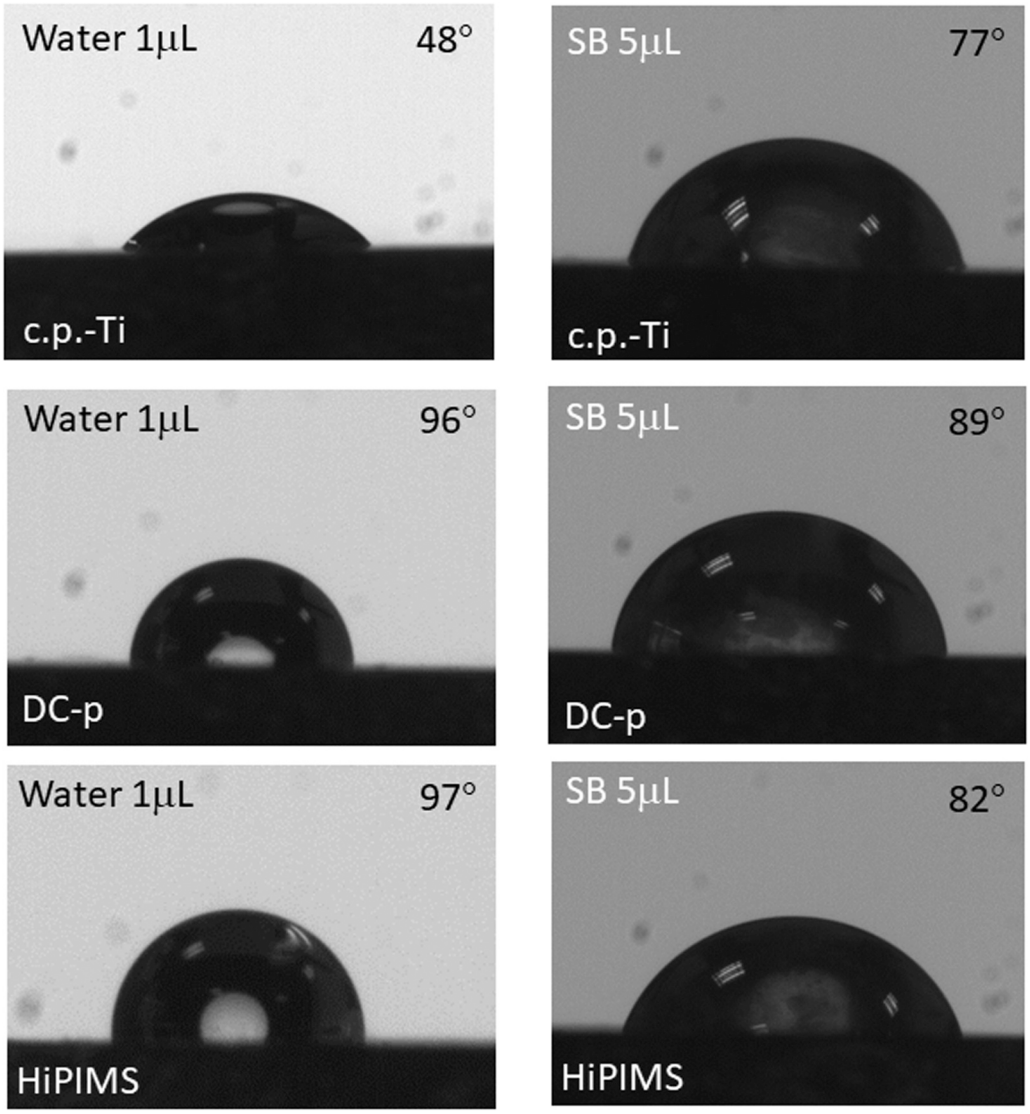

Fig. 8. Contact angle measurements on the coated surfaces using water and bovine albumin serum as fluids.

by the assembly of columns of different sizes with open inter-columnar boundaries as observed by the SEM micrographs. It is worth mentioning that nanoscale and surface effects influence the mechanical properties measured by nanoindentation giving higher values than those typical of bulk materials. For instance, common E values of c.p.-Ti and Ti6Al4V are found to be around 105–110 GPa. In conclusion, the deposition of a thin film of Ti6Al4V alloy by means of HiPIMS enables the enhancement of the surface mechanical properties (higher H/E and H^3/E^2 values) while maintaining a lighter titanium core, which results very attractive for dental implants.

The chemistry of the surfaces has also a strong effect on the surface energy of materials and thus on their wettability and the consequent interaction with the environment. XPS analysis carried out on the coated specimens revealed that the atomic titanium concentrations were almost twice that of the pristine surface (~7 at.% and 8 at.% for DC-p and HiPIMS respectively versus ~4 at.% of the substrate). No signal of vanadium could be detected at the outmost part of the surface (Survey spectrum presented in Supporting information Fig. S1). The absence of vanadium on the coatings' surface would ensure a low cytotoxicity and its potential biofunctionality[37,38]. Fig. 7 exhibits comparatively the O 1s and Ti 2p photoelectron peaks for each type of coating. In addition, the surface aluminum content has been found to be around 2 at.% where the metallic character prevails at the surface with a small oxidized contribution for both coatings (see Fig. S1 in Supporting information). HiPIMS process leads to higher surface titanium concentration predominantly in oxidized state (metallic Ti-Ti bond formation at the surface has not been observed) [39–41]. In accordance, two main components can be distinguished in the O 1s resolved photoelectron spectra: the most intense Ti-O (~530 eV) contribution and the secondary Ti-OH (~533 eV) one attributed to the oxygen and water adsorption on the surface. A small contribution of Al-O bond was also considered in agreement with the results of Fig. S1 for Al 2p peak. The formation of a TiO_2 surface layer is known to be a high protective barrier against corrosion in contact with biofluids [42], as well as to favor the osseointegration process notably in nanostructured surfaces [43].

Wettability of the implant surfaces has a strong effect on the biological system: adhesion of proteins, interaction of the surfaces with hard and soft tissue cells, affinity for bacteria and biofilm formation. The wetting properties of bare and coated substrates were studied using contact angle measurements with water and bovine albumin serum as simulated biological media (results on Fig. 8). The wettability of the surfaces demonstrates an increase of the contact angle after the coating deposition (from 48° to 80–100°), both with water and bovine serum, indicating a hydrophobic character, as it is

known from literature [26,39,44]. Although hydrophilic surfaces tend to favor the early stages of cell adhesion, proliferation and differentiation, hydrophobic surfaces are reported to absorb more protein with respect to hydrophilic ones affecting not only the amount of proteins absorbed but also their spatial distribution [2,26,44]. Previous works have presented hydrophobic dental implants as protective barriers against biodegradation induced by water and waterbone agents [45], particularly, with bacteria of acidic character. Moreover, as hydrophobic surfaces in contact with water become usually negatively charged, they are generally more resistant to negatively charged bacterial colonization. Thus, microorganisms generally adhere less to a hydrophobic substrate because a material of lower surface energy weakens the bacteria-surface adhesion [46].

This wetting behavior can be related with the induced changes at the surface, both at topographical and chemical levels previously discussed. Even when the average surface roughness values are of the same order before and after coating deposition for both type of coatings (cf. Fig. 4), the surface morphology shows clear differences as demonstrated by SEM observation and statistical image analysis, evidencing a surface nanostructuring that changes the wetting behavior. Surface modification by the introduction of micro and nanoscale features, trying to mimic the bone's hierarchical structure, is one of the current trends to improve osseointegration [43] and the success of commercial implants [44]. Current works have revealed that osteoblasts, through cytoskeletal organization and spread morphology, are more sensible to surface topography changes than to surface wettability modification [47]. Nanoscaled surfaces have been demonstrated to favor protein adsorption required for the osteogenic cell migration [42]. Additionally, nanostructured hydrophobic surfaces are a current strategy to difficult the bacteria adsorption and growth as an alternative to the widespread and excessive use of antibiotics [48,49] taking advantages of the difference in size between bacteria and living tissue cells such as osteoblasts (i.e., several micrometers compared to a few tens of microns, respectively). It has been found a considerable reduction of bacterial colonization of titanium surfaces as the number of adhesion sites and exposed area decreased due to an enhanced nanoroughness [50,51]. Furthermore, porous surfaces with pore diameter in the order of 70 nm have been found as osteoconductivity trigger systems [37]. In view of the observed average nanoroughness values in the coated surfaces both with HiPIMS and DC-p, with mean column and pore dimensions below 50 nm, the surface topography appears "smooth" from the osteoblast's well proliferation dimension [52] but can potentially affect the bacterial development. The present results place pulsed magnetron sputtering technology as a good strategy to tune surface properties of Ti implants and further bioactivity studies are foreseen.

4. Conclusions

Pulsed magnetron sputtering technologies (HiPIMS and DC-p) have been used to tune satisfactorily the bio-interface in pure Ti specimens prepared by powder metallurgy using Ti6Al4V alloy as coating material. The films with thicknesses in the range of 1–3 µm were characterized to be dense, conformal and adherent to the Ti surfaces developing a typical nanoroughness with average values below 50 nm. The mechanical properties were improved in the case of the novel HiPIMS technology leading to higher hardness ($H \approx 8$ GPa), elastic strain to failure ($H/E = 0.05$) and resistance to plastic deformation ($H^3/E^2 = 0.019$) in comparison with the bare substrate. The formation of a TiO_2 surface protective layer can help to prevent corrosion in biological media. Both coated surfaces were found to be hydrophobic, which could be related to the surface nanostructuring and chemical functionalization, what is expected to improve the antibacterial effect. The combination of surface architecture (*smooth* for bone cells and *rough* for bacteria) with low surface energy and improved mechanical performance qualify the surface modification of implants by the novel HiPIMS technology as a promising strategy to have a good compromise between bio and mechanical properties, both of extreme importance for the medical applications.

CRediT authorship contribution statement

J.C. Sánchez-López: Concept, Methodology, Resources, Writing Review & Editing, Project administration, Funding acquisition**. M. Rodríguez-Albelo:** Investigation, Visualization. **M. Sánchez-P é rez:** Investigation, Visualization. **V. Godinho:** Investigation, Visualization, Writing - Original Draft. **C. López-Santos:** Investigation, Visualization, Funding acquisition. **Y. Torres:** Concept, Methodology, Resources, Writing Review & Editing, Project administration, Funding acquisition**.**

Data availability

Data will be made available on request.

Declaration of Competing Interest

The authors declare that they have no known competing financial interests or personal relationships that could have appeared to influence the work reported in this paper.

Acknowledgments

European Regional Development Funds program (EU-FEDER) and Junta de Andalucía (PAIDI2020 project no. US-1259771 and P18-RT-2641) are acknowledged for financial support. SEM and XRD service analysis at the Instituto de Ciencia de Materiales de Sevilla are also acknowledged. C.L.-S. thanks the support of the University of Seville through the VI PPIT-US and the Ramon y Cajal Spanish National programs funded by MCIN/AEI/ 10.13039/501100011033.

Appendix A. Supporting information

Supplementary data associated with this article can be found in the online version at doi:10.1016/j.jallcom.2023.170018.

References

[1] D. Buser, S.F.M. Janner, J.-G. Wittneben, U. Brägger, C.A. Ramseier, G.E. Salvi, 10-year survival and success rates of 511 titanium implants with a sandblasted and acid-etched surface: a retrospective study in 303 partially edentulous patients, Clin. Implant Dent. Relat. Res. 14 (2012) 839–851.
[2] G. Zhu, G. Wang, J.J. Li, Advances in implant surface modifications to improve osseointegration, Mater. Adv. 2 (2021) 6901–6927.
[3] Q. Wang, P. Zhou, S. Liu, S. Attarilar, R.L.-W. Ma, Y. Zhong, L.J.N. Wang, Multi-scale surface treatments of titanium implants for rapid osseointegration: a review, Nanomaterials 10 (2020) 1244.
[4] C. García-Cabezón, V. Godinho, C. Salvo-Comino, Y. Torres, F. Martín-Pedrosa, Improved corrosion behavior and biocompatibility of porous titanium samples coated with bioactive chitosan-based nanocomposites, Materials 14 (2021).
[5] A.M. Beltrán, M. Giner, Á. Rodríguez, P. Trueba, L.M. Rodríguez-Albelo, M.A. Vázquez-Gámez, V. Godinho, A. Alcudia, J.M. Amado, C. López-Santos, Y. Torres, Influence of femtosecond laser modification on biomechanical and biofunctional behavior of porous titanium substrates, Materials 15 (2022).
[6] B. Begines, C. Arevalo, C. Romero, Z. Hadzhieva, A.R. Boccaccini, Y. Torres, Fabrication and characterization of bioactive gelatin-alginate-bioactive glass composite coatings on porous titanium substrates, ACS Appl. Mater. Interfaces 14 (2022) 15008–15020.
[7] A.M. Beltrán, B. Begines, A. Alcudia, J.A. Rodríguez-Ortiz, Y. Torres, Biofunctional and tribomechanical behavior of porous titanium substrates coated with a bioactive glass bilayer (45S5–1393), ACS Appl. Mater. Interfaces 12 (2020) 30170–30180.
[8] E. Frutos, M. Karlik, T. Polcar, The role of α'' orthorhombic phase content on the tenacity and fracture toughness behavior of Ti-22Nb-10Zr coating used in the design of long-term medical implants, Appl. Surf. Sci. 464 (2019) 328–336.

[9] V. Godinho, T.C. Rojas, A. Fernandez, Magnetron sputtered a-SiOxNy thin films: a closed porous nanostructure with controlled optical and mechanical properties, Microporous Mesoporous Mater. 149 (2012) 142–146.
[10] T.C. Rojas, A. Caro, G. Lozano, J.C. Sánchez-López, High-temperature solar-selective coatings based on Cr(Al)N. Part 1: microstructure and optical properties of CrNy and Cr1-xAlxNy films prepared by DC/HiPIMS, Sol. Energy Mater. Sol. Cells 223 (2021) 110951.
[11] L. Minati, C. Migliaresi, L. Lunelli, G. Viero, M. Dalla Serra, G. Speranza, Plasma assisted surface treatments of biomaterials, Biophys. Chem. 229 (2017) 151–164.
[12] P.K. Chu, J.Y. Chen, L.P. Wang, N. Huang, Plasma-surface modification of biomaterials, Mater. Sci. Eng.: R: Rep. 36 (2002) 143–206.
[13] D. Xie, L.J. Wei, H.Y. Liu, K. Zhang, Y.X. Leng, D.T.A. Matthews, R. Ganesan, Y.Y. Su, Deposition of titanium films on complex bowl-shaped workpieces using DCMS and HiPIMS, Surf. Coat. Technol. 442 (2022) 128192.
[14] J. Alami, Z. Maric, H. Busch, F. Klein, U. Grabowy, M. Kopnarski, Enhanced ionization sputtering: a concept for superior industrial coatings, Surface and Coatings Technology, Surf. Coat. Technol. 255 (2014) 43–51.
[15] J.C. Oliveira, F. Ferreira, A. Anders, A. Cavaleiro, Reduced atomic shadowing in HiPIMS: role of the thermalized metal ions, Appl. Surf. Sci. 433 (2018) 934–944.
[16] A. Anders, Y. Yang, Plasma studies of a linear magnetron operating in the range from DC to HiPIMS, J. Appl. Phys. 123 (2018) 043302.
[17] K. Sarakinos, J. Alami, S. Konstantinidis, High power pulsed magnetron sputtering: a review on scientific and engineering state of the art, Surf. Coat. Technol. 204 (2010) 1661–1684.
[18] J.T. Gudmundsson, J. Fischer, B.P. Hinriksson, M. Rudolph, D. Lundin, Ionization region model of high power impulse magnetron sputtering of copper, Surf. Coat. Technol. 442 (2022) 128189.
[19] S. Rtimi, O. Baghriche, C. Pulgarin, A. Ehiasarian, R. Bandorf, J. Kiwi, Comparison of HIPIMS sputtered Ag- and Cu-surfaces leading to accelerated bacterial inactivation in the dark, Surf. Coat. Technol. 250 (2014) 14–20.
[20] A. Anders, A structure zone diagram including plasma-based deposition and ion etching, Thin Solid Films 518 (2010) 4087–4090.
[21] S. Schiller, K. Goedicke, J. Reschke, V. Kirchhoff, S. Schneider, F. Milde, Pulsed magnetron sputter technology, Surf. Coat. Technol. 61 (1993) 331–337.
[22] W.-Y. Wu, M.-Y. Chan, Y.-H. Hsu, G.-Z. Chen, S.-C. Liao, C.-H. Lee, P.-W. Lui, Bioapplication of TiN thin films deposited using high power impulse magnetron sputtering, Surf. Coat. Technol. 362 (2019) 167–175.
[23] S.-C. Liao, C.-Y. Chen, Y.-H. Hsu, C.-T. Li, C.-C. Hsieh, M.-S. Tsai, M.-Y. Chan, C.-H. Lee, S.-H. Wang, S.-K. Ng, In vitro and in vivo biocompatibility study of surface modified TiN deposited on Ti6Al4V using high-power impulse magnetron sputtering technique, Surf. Coat. Technol. 394 (2020) 125814.
[24] A.A. Sugumaran, Y. Purandare, K. Shukla, I. Khan, A. Ehiasarian, P. Hovsepian, TiN/NbN nanoscale multilayer coatings deposited by high power impulse magnetron sputtering to protect medical-grade CoCrMo alloys, Coatings 11 (2021) 867.
[25] M.F. Kunrath, T.C. Muradás, N. Penha, M.M. Campos, Innovative surfaces and alloys for dental implants: what about biointerface-safety concerns? Dent. Mater. 37 (2021) 1447–1462.
[26] J. Barberi, S. Spriano, Titanium and protein adsorption: an overview of mechanisms and effects of surface features, Materials 14 (2021) 1590.
[27] A.N. Aufa, M.Z. Hassan, Z. Ismail, Recent advances in Ti-6Al-4V additively manufactured by selective laser melting for biomedical implants: prospect development, J. Alloy. Compd. 896 (2022) 163072.
[28] P. Szymczyk-Ziółkowska, G. Ziółkowski, V. Hoppe, M. Rusińska, K. Kobiela, M. Madeja, R. Dziedzic, A. Junka, J. Detyna, Improved quality and functional properties of Ti-6Al-4V ELI alloy for personalized orthopedic implants fabrication with EBM process, J. Manuf. Process. 76 (2022) 175–194.
[29] W.C. Oliver, G.M. Pharr, An improved technique for determining hardness and elastic modulus using load and displacement sensing indentation experiments, J. Mater. Res. 7 (1992) 1564–1583.
[30] H. Elmkhah, F. Attarzadeh, A. Fattah-alhosseini, K.H. Kim, Microstructural and electrochemical comparison between TiN coatings deposited through HIPIMS and DCMS techniques, J. Alloy. Compd. 735 (2018) 422–429.
[31] A. Ferrec, J. Kéraudy, P.-Y. Jouan, Mass spectrometry analyzes to highlight differences between short and long HiPIMS discharges, Appl. Surf. Sci. 390 (2016) 497–505.
[32] Y. Gaillard, E. Jiménez-Piqué, M.J.P.M. Anglada, Scale dependence of the Young's modulus measured by nanoindentation in columnar YSZ EB-PVD thermal barriers coatings, Phil. Mag. A 86 (2006) 5441–5451.
[33] A. Leyland, A. Matthews, On the significance of the H/E ratio in wear control: a nanocomposite coating approach to optimised tribological behaviour, Wear 246 (2000) 1–11.
[34] M.-K. Han, J.-B. Im, M.-J. Hwang, B.-J. Kim, H.-Y. Kim, Y.-J. Park, Effect of indium content on the microstructure, mechanical properties and corrosion behavior of titanium alloys, Metals 5 (2015) 850–862.
[35] M. Samuelsson, D. Lundin, J. Jensen, M.A. Raadu, J.T. Gudmundsson, U. Helmersson, On the film density using high power impulse magnetron sputtering, Surf. Coat. Technol. 205 (2010) 591–596.
[36] D. Kümmel, D. Linsler, R. Schneider, J. Schneider, Surface engineering of a titanium alloy for tribological applications by nanosecond-pulsed laser, Tribol. Int. 150 (2020) 106376.
[37] K. Satoh, N. Ohtsu, S. Sato, K. Wagatsuma, Surface modification of Ti–6Al–4V alloy using an oxygen glow-discharge plasma to suppress the elution of toxic elements into physiological environment, Surf. Coat. Technol. 232 (2013) 298–302.
[38] S. Guan, M. Qi, C. Wang, S. Wang, W. Wang, Enhanced cytocompatibility of Ti6Al4V alloy through selective removal of Al and V from the hierarchical micro-arc oxidation coating, Appl. Surf. Sci. 541 (2021) 148547.
[39] J. Vaithilingam, S. Kilsby, R.D. Goodridge, S.D.R. Christie, S. Edmondson, R.J.M. Hague, Functionalisation of Ti6Al4V components fabricated using selective laser melting with a bioactive compound, Mater. Sci. Eng.: C. 46 (2015) 52–61.
[40] M. Hornschuh, P. Zwicker, T. Schmidt, B. Finke, A. Kramer, G. Müller, Poly (hexamethylene biguanide), adsorbed onto Ti-Al-V alloys, kills slime-producing Staphylococci and Pseudomonas aeruginosa without inhibiting SaOs-2 cell differentiation, J. Biomed. Mater. Res. Part B: Appl. Biomater. 108 (2020) 1801–1813.
[41] P. Yi, L. Peng, J. Huang, Multilayered TiAlN films on Ti6Al4V alloy for biomedical applications by closed field unbalanced magnetron sputter ion plating process, Mater. Sci. Eng.: C 59 (2016) 669–676.
[42] J.C.M. Souza, M.B. Sordi, M. Kanazawa, S. Ravindran, B. Henriques, F.S. Silva, C. Aparicio, L.F. Cooper, Nano-scale modification of titanium implant surfaces to enhance osseointegration, Acta Biomater. 94 (2019) 112–131.
[43] B. Wu, Y. Tang, K. Wang, X. Zhou, L. Xiang, Nanostructured titanium implant surface facilitating osseointegration from protein adsorption to osteogenesis: the example of TiO(2) NTAs, Int J. Nanomed. 17 (2022) 1865–1879.
[44] R.A. Gittens, L. Scheideler, F. Rupp, S.L. Hyzy, J. Geis-Gerstorfer, Z. Schwartz, B.D. Boyan, A review on the wettability of dental implant surfaces II: Biological and clinical aspects, Acta Biomater. 10 (2014) 2907–2918.
[45] D.G. Moussa, A. Fok, C. Aparicio, Hydrophobic and antimicrobial dentin: a peptide-based 2-tier protective system for dental resin composite restorations, Acta Biomater. 88 (2019) 251–265.
[46] T. Sang, Z. Ye, N.G. Fischer, E.P. Skoe, C. Echeverría, J. Wu, C. Aparicio, Physical-chemical interactions between dental materials surface, salivary pellicle and Streptococcus gordonii, Colloids Surf. B: Biointerfaces 190 (2020) 110938.
[47] K. Rabel, R.-J. Kohal, T. Steinberg, B. Rolauffs, E. Adolfsson, B. Altmann, Human osteoblast and fibroblast response to oral implant biomaterials functionalized with non-thermal oxygen plasma, Sci. Rep. 11 (2021) 17302.
[48] S.W. Lee, K.S. Phillips, H. Gu, M. Kazemzadeh-Narbat, D. Ren, How microbes read the map: effects of implant topography on bacterial adhesion and biofilm formation, Biomaterials 268 (2021) 120595.
[49] A. Tripathy, P. Sen, B. Su, W.H. Briscoe, Natural and bioinspired nanostructured bactericidal surfaces, Adv. Colloid Interface Sci. 248 (2017) 85–104.
[50] P. Liu, Y. Hao, Y. Zhao, Z. Yuan, Y. Ding, K. Cai, Surface modification of titanium substrates for enhanced osteogenetic and antibacterial properties, Colloids Surf. B: Biointerfaces 160 (2017) 110–116.
[51] G. Mendonça, D.B.S. Mendonça, L.G.P. Simões, A.L. Araújo, E.R. Leite, W.R. Duarte, F.J.L. Aragão, L.F. Cooper, The effects of implant surface nanoscale features on osteoblast-specific gene expression, Biomaterials 30 (2009) 4053–4062.
[52] T.P. Kunzler, T. Drobek, M. Schuler, N.D. Spencer, Systematic study of osteoblast and fibroblast response to roughness by means of surface-morphology gradients, Biomaterials 28 (2007) 2175–2182.